Molecular Spin-Flip Loss and a Dual Quadrupole Trap

David Reens,* Hao Wu,* Tim Langen,† and Jun Ye
JILA, National Institute of Standards and Technology and the University of Colorado and Department of Physics, University of Colorado, Boulder, Colorado 80309-0440, USA
(Dated: September 25, 2017)

Doubly dipolar molecules exhibit complex internal spin-dynamics when electric and magnetic fields are both applied. Near magnetic trap minima, these spin-dynamics lead to enhancements in Majorana spin-flip transitions by many orders of magnitude relative to atoms, and are thus an important obstacle for progress in molecule trapping and cooling. We conclusively demonstrate and address this with OH molecules in a trap geometry where spin-flip losses can be tuned from over 200 s^{-1} to below our 2 s^{-1} vacuum limited loss rate with only a simple external bias coil and with minimal impact on trap depth and gradient.

The ultracold regime extends toward molecules on many fronts [1]. Weakly bound dimers have been condensed [2–4], and ground state alkali dimers continue to progress, both homogeneous [5, 6] and hetereogeneous [7–11]. KRb polar molecules have reached lattice quantum degeneracy [12]. Recently developed laser cooling strategies are tackling certain nearly vibrationally diagonal molecules [13–18]. A diverse array of alternative strategies have succeeded on other molecules [19–25]. Many of these molecules will require secondary strategies like evaporation or sympathetic cooling to make further gains in phase space density [26–28]. They also may face a familiar challenge: spin flip loss near the zero of a magnetic trap, but dramatically enhanced for doubly dipolar molecules due to their internal spin dynamics in mixed electric and magnetic fields.

Spin flips were directly observed near 50 μK and overcome with a time-orbiting potential trap [29] and a plugged dipole trap [30], famously enabling the first production of Bose-Einstein condensates. Molecules produced by associated of ultracold atoms inherit the trap-plugging strategy employed for the atoms, but for directly cooled molecules this is not the case. Many direct cooling experiments begin at modest temperatures and require trap strengths typically only attained with quadrupole fields [19, 31–33]. In the 2 T/cm magnetic quadrupole used in our previous studies of hydroxyl radicals (OH) [27], spin-flips should not have had a significant influence until the μK regime, but the application of electric field changes this. Electric fields applied to magnetically trapped dipolar species offer interesting opportunities to study anisotropic collisions and quantum chemistry, as we have previously pursued [34]. They can also be useful for control over state purity [35]. But the electric field can also dramatically amplify spin-flip losses, due to internal spin-dynamics that we corroborate with direct experimental evidence for the first time in the present work. We achieve this with a novel trap geometry that also allows complete plugging of the loss with minimal sacrifice of trap strength.

The internal spin-dynamics leading to spin-flip enhancement are subtle, having eluded two previous investigations: In Ref. [36] the analogues of atomic spin-flip loss for molecules in mixed fields were modeled. It was incorrectly concluded that no significant loss enhancement due to electric field would be evident; this holds only for the approximate Hamiltonian used in that study. In Ref. [37] it was correctly noted that Hund's case (a) molecules maintain a quantization axis in mixed fields. The states of the molecule were shown to align with one of the two quantization axes given by the vectors $d_{\rm eff}\vec{E} \pm \mu_{\rm eff}\vec{B}$ [38], $\mu_{\rm eff}$ and $d_{\rm eff}$ the effective dipole moments of the molecule

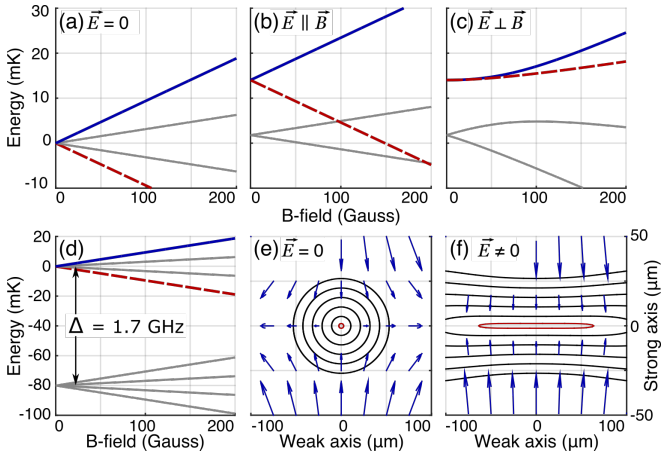

FIG. 1. A uniform electric field, added to magnetically trapped molecules for dipolar studies or other purposes, can lead to spin-flip losses. Four Zeeman split lines in OH's $X^2\Pi_{3/2}$ manifold are shown (a-c), with the doubly stretched state in blue and its spin-flip partner in dashed red. These states are shown with no electric field (a), with $|\vec{E}| = 150$ V/cm and $\vec{E} \parallel \vec{B}$ (b), and with $\vec{E} \perp \vec{B}$ (c). Note the vastly reduced red-blue splitting in the latter case. An opposite parity electrically strong field seeking manifold sits Δ below (d). Energy splitting contours are shown every 40 MHz near the zero of a 2 T/cm magnetic quadrupole trap for OH molecules [35] with $\vec{E} = 0$ (e), and with uniform $E = 150$ V/cm along the strong axis of the quadrupole (f). The vectors are $d_{\rm eff}\vec{E} + \text{sign}(\vec{E} \cdot \vec{B})\mu_{\rm eff}\vec{B}$, the proper quantization axis for well-trapped molecules as described in the text. Note the drastic widening of the lowest contour (red), the culprit for molecular spin-flip loss enhancement.

in uncombined fields. The key idea is that Hund's case (a) molecules have both dipole moments fixed to their internuclear axis, so that in the molecular frame, the energy shifts from the two fields combine like vectors. It was asserted that this would maintain quantization near the zero of a quadrupole trap and avoid spin-flip loss, but as we now describe, the loss is actually enhanced.

We begin with an intuitive picture. In order to remain well-trapped in combined fields, a molecule must remain weak field seeking with respect to both fields, i.e. doubly stretched. But in a geometry where the fields are continuously rotating, the quantization axis that defines the doubly stretched state can be either of $d_{\rm eff}\vec{E} \pm \mu_{\rm eff}\vec{B}$, depending on whether the fields are oriented closer to parallel or antiparallel. Consider a molecule initially in the hemisphere of a quadrupole trap where the fields are close to parallel and in the doubly stretched state with the sum quantization axis $d_{\rm eff}\vec{E} + \mu_{\rm eff}\vec{B}$. If its trajectory carries it near the trap center where the magnetic field is small, the electric field does indeed maintain the quantization axis. However, because the magnetic field orientation also changes near the center, the molecule enters the hemisphere where the fields are closer to antiparallel. The length of the quantization axis, which is proportional to the field induced energy shift of the molecule, now decreases in magnitude with increasing magnetic field. This molecule is now magnetically strong field seeking and will be lost. Thus the doubly stretched state is degenerate with a magnetically strong field seeking spin-flip partner state wherever the electric and magnetic fields are orthogonal, at least in this intuitive first order picture. Defining $\phi = \vec{E} \cdot \vec{B}$ the field orientation, the well-trapped molecule most have the quantization axis $d_{\rm eff}\vec{E} + {\rm sign}(\phi)\mu_{\rm eff}\vec{B}$. Since ϕ is a continuous scalar, $\phi = 0$ is its contour level and always corresponds to a 2D surface; in a magnetic quadrupole with homogeneous electric field it is a plane.

This intuition agrees with a more rigorous analysis of the energy splitting G between the trapped state and its spin-flip partner. By diagonalizing the approximate eight state ground molecular Hamiltonian for OH, subtracting the relevant state energies and Taylor expanding, we find:

$$G(\mathcal{B}_\perp, \mathcal{B}_{||}, \mathcal{E}) = \mathcal{B}_{||} + \mathcal{B}_\perp^3 \frac{\Delta^2}{\mathcal{E}^4} + \mathcal{O}(\mathcal{B}_{||}^2, \mathcal{B}_\perp^4) \qquad (1)$$

Here $\mathcal{B}_{\perp,||} = \mu_{\rm eff}\vec{B} \cdot \hat{e}_{\perp,||}$, where $\hat{e}$ is the unit vector in the labeled direction relative to the electric field. $\mathcal{E} = |d_{\rm eff}\vec{E}|$, Δ is the lambda doubling, and G is the energy gap between the trapped state and its spin-flip partner. The relevant splitting is not quite zero where $\vec{E} \perp \vec{B}$ and $B_{||} = 0$ thanks to Δ, but nonetheless reaches a deep minimum; the remaining Zeeman splitting is reduced from linear to cubic in magnetic field (Fig. 1). This Zeeman splitting suppression is in fact a known phenomenon in the precision measurement community [39, 40], and experimentalists have exploited it to suppress the influence of magnetic fields in electron EDM measurements. However, in the case of applying mixed fields during trapping, this suppression is not beneficial but rather detrimental.

TABLE I. Enhancements (η) and loss rates (γ) for OH with typical applied fields. Zero field values are equivalent to traditional spin-flip loss. Electric field is required during evaporation and spectroscopy to open avoided crossings [27, 35], or applied to polarize the molecules and study collisions [34].

E (V/cm)	55 mK		5 mK		Purpose
	η	$\gamma\,(s^{-1})$	η	$\gamma\,(s^{-1})$	
0	1	0.02	1	1.3	Zero Field
300	5	0.1	9	11	Evaporation
550	17	0.3	40	50	Spectroscopy
3000	1000	19	1600	2000	Polarizing

To deduce the effect of this loss plane on the ensemble, we consider molecular trajectories in light of the Landau Zener formula:

$$P_{\rm hop} = e^{-\delta^2/\hbar\dot{G}}, \qquad (2)$$

which relates the probability of diabatically hopping between two states $P_{\rm hop}$ to their energetic coupling δ and their rate of approach $\dot{G} = v_z dG/dz$. Here z and v_z are normal to the $\vec{E} \perp \vec{B}$ plane, and we neglect the components of $\dot{G}$ due to the other coordinates since from Eqn. 1 it is clear that G grows predominately in one direction. We can also set δ to the minimum energy gap along the trajectory, which is found in the plane. This facilitates direct numerical computation of loss rates by integrating the molecule flux through the plane for a thermal distribution, weighted by the hopping probability. We perform these integrations for OH in a 2 T/cm magnetic quadrupole [41] under various electric fields (Tab. I).

It is also possible to proceed algebraically so as to develop a scaling law. This yields the electric field induced loss enhancement factor

$$\eta = \left(\frac{d_{\rm eff}E}{\sqrt{\kappa\Delta}}\right)^{8/3}, \qquad (3)$$

see Sec. 3 of [42] for the full derivation. Here κ is a characteristic energy scale for spin-flips that can be derived by setting $P_{\rm hop} = 1/e$ in Eqn. 2 and solving for δ. This means that for electric fields with $d_{\rm eff}E > \sqrt{\kappa\Delta}$, the loss enhancement is almost cubic with electric field. Crucially, it is not Δ that sets the relevant scale, as one might naively suppose given that this is the energy beyond which the Stark effect is linear and the molecule is polarized. Instead it is $\sqrt{\kappa\Delta}$, which is in general much smaller; $\kappa = 5$ MHz for OH in our trap, while $\Delta = 1.7$ GHz.

Returning to the numerical approach, the direct integration of flux is a key improvement relative to our previous work [34], where electric fields were applied to study collisions. The mechanism of molecular spin-flip loss was

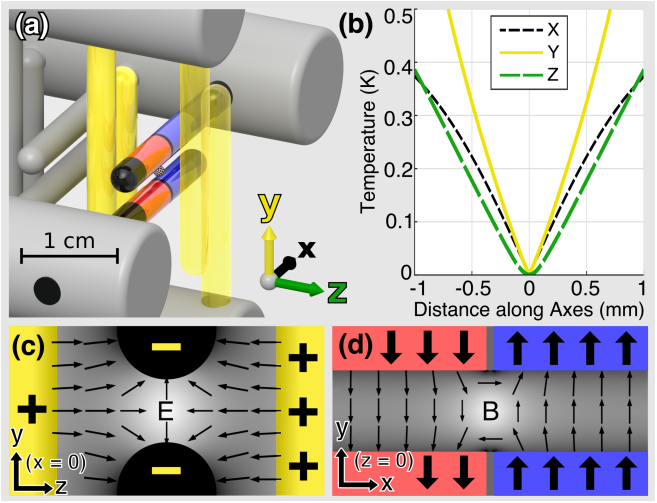

FIG. 2. The last six pins of our Stark decelerator [41] form the trap (a), which is 0.45 K deep with trap frequency $\nu \approx 4$ kHz (b). Along y the trap is bounded by the 2 mm pin spacing. The yellow pins are positively charged and the central pin pair negatively, which forms a 2D electric quadrupole trap with zero along the x-axis. This is shown for the $x = 0$ plane (c), with yellow pins artificially projected for clarity since they don't actually intersect the plane. The central pins are magnetized, with two domains each. Blue indicates magnetization along $+\hat{y}$, red along $-\hat{y}$. These domains produce a magnetic quadrupole trap with zero along the z-axis, shown in the $z = 0$ plane (d).

identified, and an attempt was made to deconvolve it from the collisional effect of the electric field. Revisiting this with the direct integration of flux, we find a threefold larger loss magnitude, enough to explain a significant portion of the effect previously attributed to collisions, see Sec. 1 of our supplementary materials [42]. In light of this, it becomes especially important to perform direct, unconvolved experimental verification of both the magnitude of the loss effect and the validity of our loss-flux calculations. We now present a new trap where this is achieved.

Our idea is to use a pair of 2D quadrupole traps, one magnetic and the other electric, with orthogonal centerlines (Fig. 2):

$$\vec{B} = B'x\hat{y} - B'y\hat{x} \qquad \vec{E} = E'y\hat{y} - E'z\hat{z} \tag{4}$$

We achieve these fields in a geometry that matches our Stark decelerator [21]. This geometry features large spin-flip loss, since $\vec{E} \perp \vec{B}$ in both the $x = 0$ and $y = 0$ planes, and from Eqn. 1, $G = \mathcal{B}_\perp^3 \Delta^2 / \mathcal{E}^4$ will be generally very small due to the large $\mathcal{E}$. However, by adding a small magnetic field $\vec{B} = B_{\text{coil}}\hat{z}$ along the centerline of the magnetic quadrupole with an external bias coil, a dramatic change can be made to the surfaces where $\vec{E} \perp \vec{B}$ with minimal perturbation of the trapping potential.

B_{coil} morphs the $\vec{E} \perp \vec{B}$ surface from a pair of planes into the hyperbolic sheet given by $x \cdot y = z \cdot B_{\text{coil}}/B'$

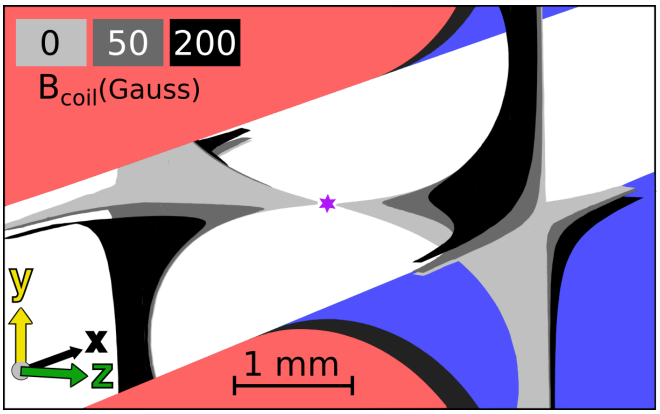

FIG. 3. Surfaces where spin-flips can occur are shown for three values of B_{coil} in light gray, dark gray, and black. The magnetic pins are shown as in Fig. 2 for context. The purple star marks the trap center, to which molecules are confined within a ~1 mm diameter.

(Substitute Eqn. 4 into $\vec{E} \cdot \vec{B} = 0$). This means that $\vec{E} \perp \vec{B}$ is pushed away from the z-axis where $\vec{B}$ is smallest. In Fig. 3, the surfaces where $\vec{E} \perp \vec{B}$ for several B_{coil} magnitudes are calculated and shown wherever $G \leq \kappa$. The loss regions ought to be tuned far enough from the trap center that molecules cannot access them. This is indeed what we observe, note the striking difference in trap lifetimes in Fig. 4a. With only 200 G bias field (the trap is 5 kG deep) the loss is suppressed below that due to background gas.

In order to further verify our calculations of loss by integration of molecule fluxes across $\vec{E} \perp \vec{B}$ surfaces, we perform these calculations for a diverse collection of loss surfaces obtained by translation of the magnetic pins in their mounts. This translation disrupts the idealized 2D magnetic quadrupole by adding a small trapping field $\vec{B} \propto B'z\hat{z}$, which significantly alters the topology of the $\vec{E} \perp \vec{B}$ surface and the overall loss rate in the trap. We perform this translation in situ, and obtain a reasonable agreement (Fig. 4b). This is particularly noteworthy given that the direct integral calculation assumes a purely thermal distribution and doesn't involve the computation of any actual trajectories. The only free parameter is temperature, which enters the calculation via the thermal distribution used for integration, and fits to 170 ± 20 mK [43]. An intuitive explanation for the intriguing double well structure in population verses B_{coil} is that B_{coil} first translates the magnetic zero along the z-axis, overlapping it with larger electric fields at first before moving it out of the trap.

With strong experimental confirmation of the molecular spin-flip loss enhancement, we can move on to generalize beyond OH. Hund's case (a) states are most susceptible in the sense that smaller electric fields are sufficient to cause a significant problem, but with enough electric field any state exhibiting competition between

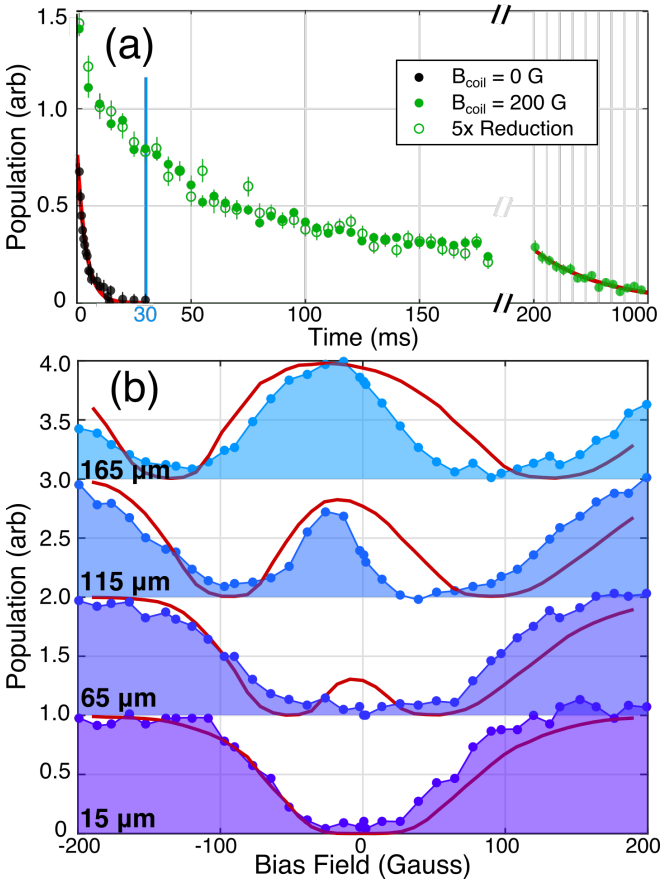

FIG. 4. Time traces (a) without bias field (black), with bias field (green dots), and with modulated density (green circles). One body fits (red) give loss rates of 200 s^{-1} without bias field and 2 s^{-1} with full bias field at long times, in agreement with our background gas pressure. At the fixed time 30 ms, population is shown as a function of both pin translation and bias field (b), for several values of pin translation, labeled relative to perfect alignment. Fits (red) are calculated by integrating the molecule flux of a thermal ensemble through surfaces where $\vec{E} \perp \vec{B}$.

electric and magnetic fields for alignment of the molecule or atom will be susceptible. One way to avoid competition is for the fields to couple to unrelated parts of the Hamiltonian, which happens to a limited extent for Hund's case (b) states without electron orbital angular momentum (Σ states, $\Lambda = 0$) [37]. In these states, which include most laser-cooled molecules thus far, the electric and magnetic fields couple to rotation and spin respectively, which are only related by the spin-rotation coupling constant γ. Since γ is usually in the tens of MHz [28], molecular spin-flip loss remains quite significant. The inclusion of hyperfine requires a careful case-by-case investigation. For OH, it would initially seem to add an extra splitting that could protect from spin-flips, but in fact the loss plane is only shifted slightly away from $\vec{E} \perp \vec{B}$ and retains the same area. For YO [44], certain hyperfine states can avoid spin-flip loss entirely when electric fields are applied. These states are characterized by significant electron-spin-to-nuclear-spin dipolar coupling, which results in a protective gap regardless of field orientation.

It is also instructive to consider the related case of a pure electrostatic trap. Here there is always some zero field parity splitting that prevents the orientation-reversing spin flips we have been discussing. However, this same splitting pushes all states with the same sign of m, the field alignment quantum number, very close to one another, leading to loss via Landau-Zener transitions other than the m to $-m$ spin-flip [45]. Intriguingly, the addition of a homogeneous magnetic field can actually suppress this loss [46].

The present trap, in addition to providing the desired experimental testing ground for molecular spin-flip loss, produces large 5 T/cm trap gradients useful for maintaining high densities to facilitate collisional studies. This is in contrast with other strategies for plugging the hole of a magnetic trap which often lead to a reduction in trap gradient. With loss removed, we observe a population trend whose initially fast decay rate decreases over time (Fig. 4a, green dots), suggesting a two-body collisional effect. We test this by reducing the initial population fivefold but without changing its spatial or velocity distribution [42], and then scale the resulting trend by five (green circles). If collisions had contributed, this new trend would show less decay, but we observe no significant change. This seeming lack of collisions could be due to the warmer initial temperature of 170 mK, in contrast to the earlier work at and below 50 mK [27]. The results of this paper are important for the evaporation work, since the electric fields used for the RF knife ought to have caused a significant spin-flip loss effect, especially at low temperatures [42]. An alternative hypothesis for the population trend is the existence of chaotic trap orbits with long escape times [47]. Moving forward, we aim to increase the density by means of several improvements [48, 49].

Molecule enhanced spin-flip loss arises in mixed electric and magnetic fields due to a competition between field quantization axes. We conclusively demonstrate and suppress this effect using our dual magnetic and electric quadrupole trap, which is also an ideal setting for further progress in collisional physics thanks to its large trap gradient. Our calculation of the magnitude of spin-flip loss via flux through surfaces where $\vec{E} \perp \vec{B}$ enables detailed predictions of how its location and magnitude ought to scale with bias field and trap alignment, which we experimentally verify. Our results correct existing predictions about molecular spin-flips in mixed fields and pave the way toward further improvements in molecule trapping and cooling.

We acknowledge the Gordon and Betty Moore Foundation, the ARO-MURI, JILA PFC, and NIST for their financial support. T.L. acknowledges support from the

Alexander von Humboldt Foundation through a Feodor Lynen Fellowship. We thank J.L. Bohn, S.Y.T. van de Meerakker, and M.T. Hummon for helpful discussions. We thank Goulven Quéméner for his continued involvement in this research.

* Contributed equally. Email dave.reens@colorado.edu or hao.wu@colorado.edu.

† Present Address: 5. Physikalisches Institut and Center for Integrated Quantum Science and Technology (IQST), Universität Stuttgart, Pfaffenwaldring 57, 70569 Stuttgart, Germany

[1] L. D. Carr, D. DeMille, R. V. Krems, and J. Ye, New Journal of Physics **11**, 055049 (2009).

[2] M. Greiner, C. A. Regal, and D. S. Jin, Nature **426**, 537 (2003).

[3] M. W. Zwierlein, C. A. Stan, C. H. Schunck, S. M. F. Raupach, S. Gupta, Z. Hadzibabic, and W. Ketterle, Physical Review Letters **91**, 250401 (2003).

[4] S. Jochim, M. Bartenstein, A. Altmeyer, G. Hendl, S. Riedl, J. Hecker Denschlag, and R. Grimm, Science **302**, 2101 (2003).

[5] F. Lang, K. Winkler, C. Strauss, R. Grimm, and J. H. Denschlag, Physical Review Letters **101**, 1 (2008).

[6] J. G. Danzl, M. J. Mark, E. Haller, M. Gustavsson, R. Hart, J. Aldegunde, J. M. Hutson, and H.-C. Nägerl, Nature Physics **6**, 265 (2010).

[7] T. Takekoshi, L. Reichsöllner, A. Schindewolf, J. M. Hutson, C. R. Le Sueur, O. Dulieu, F. Ferlaino, R. Grimm, and H.-C. Nägerl, Physical Review Letters **113**, 205301 (2014).

[8] J. W. Park, S. A. Will, and M. W. Zwierlein, Physical Review Letters **114**, 205302 (2015).

[9] M. Guo, B. Zhu, B. Lu, X. Ye, F. Wang, R. Vexiau, N. Bouloufa-Maafa, G. Quéméner, O. Dulieu, and D. Wang, Physical Review Letters **116**, 205303 (2016).

[10] L. R. Liu, J. T. Zhang, Y. Yu, N. R. Hutzler, Y. Liu, T. Rosenband, and K.-K. Ni, "Ultracold Molecular Assembly," (2017), arXiv:1701.03121.

[11] T. M. Rvachov, H. Son, A. T. Sommer, S. Ebadi, J. J. Park, M. W. Zwierlein, W. Ketterle, and A. O. Jamison, "Long-Lived Ultracold Molecules with Electric and Magnetic Dipole Moments," (2017), arXiv:1707.03925.

[12] S. A. Moses, J. P. Covey, M. T. Miecnikowski, B. Yan, B. Gadway, J. Ye, and D. S. Jin, Science **350**, 659 (2015).

[13] B. K. Stuhl, B. C. Sawyer, D. Wang, and J. Ye, Physical Review Letters **101**, 243002 (2008).

[14] M. T. Hummon, M. Yeo, B. K. Stuhl, A. L. Collopy, Y. Xia, and J. Ye, Physical Review Letters **110**, 143001 (2013).

[15] J. F. Barry, D. J. McCarron, E. B. Norrgard, M. H. Steinecker, and D. DeMille, Nature **512**, 286 (2014).

[16] V. Zhelyazkova, A. Cournol, T. E. Wall, A. Matsushima, J. J. Hudson, E. A. Hinds, M. R. Tarbutt, and B. E. Sauer, Physical Review A **89**, 053416 (2014).

[17] B. Hemmerling, E. Chae, A. Ravi, L. Anderegg, G. K. Drayna, N. R. Hutzler, A. L. Collopy, J. Ye, W. Ketterle, and J. M. Doyle, Journal of Physics B: Atomic, Molecular and Optical Physics **49**, 174001 (2016).

[18] S. Truppe, H. J. Williams, M. Hambach, L. Caldwell, N. J. Fitch, E. A. Hinds, B. E. Sauer, and M. R. Tarbutt, Nature Physics (2017), 10.1038/nphys4241.

[19] J. D. Weinstein, R. DeCarvalho, T. Guillet, B. Friedrich, and J. M. Doyle, Nature **395**, 148 (1998).

[20] H. L. Bethlem, G. Berden, and G. Meijer, Physical Review Letters **83**, 1558 (1999).

[21] J. R. Bochinski, E. R. Hudson, H. J. Lewandowski, G. Meijer, and J. Ye, Physical Review Letters **91**, 243001 (2003).

[22] E. Narevicius, A. Libson, C. G. Parthey, I. Chavez, J. Narevicius, U. Even, and M. G. Raizen, Physical Review Letters **100**, 093003 (2008).

[23] A. Wiederkehr, H. Schmutz, M. Motsch, and F. Merkt, Molecular Physics **110**, 1807 (2012).

[24] A. Prehn, M. Ibrügger, R. Glöckner, G. Rempe, and M. Zeppenfeld, Physical Review Letters **116**, 063005 (2016).

[25] Y. Liu, M. Vashishta, P. Djuricanin, S. Zhou, W. Zhong, T. Mittertreiner, D. Carty, and T. Momose, Physical Review Letters **118**, 093201 (2017).

[26] L. P. Parazzoli, N. J. Fitch, P. S. Zuchowski, J. M. Hutson, and H. J. Lewandowski, Physical Review Letters **106**, 1 (2011).

[27] B. K. Stuhl, M. T. Hummon, M. Yeo, G. Quéméner, J. L. Bohn, and J. Ye, Nature **492**, 396 (2012).

[28] G. Quéméner and J. L. Bohn, Physical Review A - Atomic, Molecular, and Optical Physics **93**, 1 (2016).

[29] W. Petrich, M. H. Anderson, J. R. Ensher, and E. A. Cornell, Physical Review Letters **74**, 3352 (1995).

[30] K. B. Davis, M. O. Mewes, M. R. Andrews, N. J. van Druten, D. S. Durfee, D. M. Kurn, and W. Ketterle, Physical Review Letters **75**, 3969 (1995).

[31] J. Riedel, S. Hoekstra, W. Jäger, J. J. Gilijamse, S. Y. T. Van De Meerakker, and G. Meijer, European Physical Journal D **65**, 161 (2011).

[32] M. Quintero-Pérez, T. E. Wall, S. Hoekstra, and H. L. Bethlem, Journal of Molecular Spectroscopy **300**, 112 (2014).

[33] N. Akerman, M. Karpov, Y. Segev, N. Bibelnik, J. Narevicius, and E. Narevicius, Physical Review Letters **119**, 1 (2017).

[34] B. K. Stuhl, M. Yeo, M. T. Hummon, and J. Ye, Molecular Physics **111**, 1798 (2013).

[35] B. K. Stuhl, M. Yeo, B. C. Sawyer, M. T. Hummon, and J. Ye, Physical Review A **85**, 033427 (2012).

[36] M. Lara, B. L. Lev, and J. L. Bohn, Physical Review A **78**, 033433 (2008).

[37] J. L. Bohn and G. Quéméner, Molecular Physics **111**, 1931 (2013).

[38] The authors use $\mu_{\text{eff}}\vec{B} \pm d_{\text{eff}}\vec{E}$. We reverse this to provide a more physical connection to our experiment, where the electric field is fixed.

[39] M. A. Player and P. G. H. Sandars, Journal of Physics B: Atomic and Molecular Physics **3**, 1620 (1970).

[40] J. J. Hudson, B. E. Sauer, M. R. Tarbutt, and E. A. Hinds, Physical Review Letters **89**, 023003 (2002).

[41] B. C. Sawyer, B. K. Stuhl, D. Wang, M. Yeo, and J. Ye, Physical Review Letters **101**, 203203 (2008).

[42] See Supplementary Materials.

[43] Calculation performed in COMSOL: Source Code.

[44] This is particularly relevant given the recently realized 3D MOT for YO.

[45] T. E. Wall, S. K. Tokunaga, E. a. Hinds, and M. R.

Tarbutt, Physical Review A - Atomic, Molecular, and Optical Physics **81**, 1 (2010).

[46] S. A. Meek, G. Santambrogio, B. G. Sartakov, H. Conrad, and G. Meijer, Physical Review A - Atomic, Molecular, and Optical Physics **83** (2011), 10.1103/PhysRevA.83.033413.

[47] R. González-Férez, M. Iñarrea, J. P. Salas, and P. Schmelcher, Physical Review E **90**, 062919 (2014).

[48] U. Even, EPJ Techniques and Instrumentation **2**, 17 (2015).

[49] Y. Segev, N. Bibelnik, N. Akerman, Y. Shagam, A. Luski, M. Karpov, J. Narevicius, and E. Narevicius, Science Advances **3**, e1602258 (2017).